

Snake-like Kinematics for Minimally Invasive Surgery Using Selective Laser Sintering

*G. Horst¹⁾, M. Horper²⁾, N. Kohn²⁾, A. Fiolka¹⁾,
H. Feussner²⁾ and H. Ulbrich¹⁾

¹⁾ *Institute of Applied Mechanics, Technische Universitaet Muenchen, Germany*

²⁾ *Research Group MITI, Klinikum rechts der Isar der Technischen Universitaet
Muenchen, Germany*

¹⁾ gerald.horst@tum.de

ABSTRACT

For new instruments in Minimally Invasive Surgery, there is a need for small, miniaturized, yet dexterous and precise kinematics. Snake-like kinematics are very popular in medical products, although they are very complex and hence difficult to manufacture. Therefore, we developed a disposable bending-section manufactured by Selective Laser Sintering. This paper shows a method to design robust, precise, and adoptable snake-like kinematics that can be manufactured overnight. To show the new design's potential, a camera orientation unit for the second generation of the HVSPS was manufactured and successfully included into the system.

1. INTRODUCTION

To reduce trauma during surgery, Minimally Invasive Surgery (MIS) has become a popular alternative to open surgery. The patient can recover faster and will suffer less pain compared to standard surgery. For the laparoscopic approach, still at least three incisions in the abdominal wall are required. With novel techniques, the number of incisions can be reduced to one (Single-Port Surgery SPS) or even zero (Natural Orifice Transluminal Endoscopic Surgery NOTES). In the latter approach, entry to the abdomen is made through inner organs.

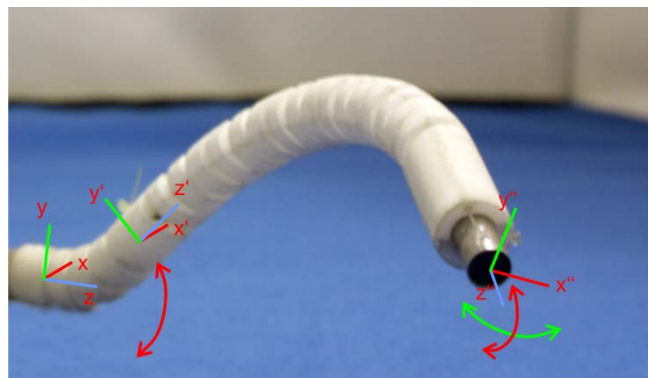


Fig. 1 prototype with mounted camera

To make use of already existing flexible instruments as they are used for endoscopic surgery, the Highly Versatile Single Port System (HVSPS) was developed by (Can 2012).

With the sigma resection being a well-known laparoscopic intervention (Weede 2012), we decided to take this as a benchmark for our system. For a laparoscopic sigma resection on a pig, (Weede 2012) showed that the instruments had to be changed up to seven times.

Not only the HVSPS makes use of snake-like kinematics. In fact, this is a very popular design for surgical devices, e.g. the IREP (Ding 2010), the commercially available Spider Surgical System, the HARP (Degani 2006), or for the systems proposed by (Peirs 2002) or (Dario2000).

These kinematics are often actuated by tendons or shape-memory-alloys (SMA). As they show a smooth bending behavior with relatively large radii, they are particularly suitable when flexible endoscopic instruments are used for tissue manipulation and have to be conducted inside the structure.

All approaches for a snake-like kinematics show a high amount of mechanical complexity and are therefore hard to adapt to different requirements, expensive to manufacture and call for an elaborate way of autoclaving. To overcome these limitations, Selective Laser Sintering (SLS) seems a good approach for cheap, adaptable, and therefore disposable kinematics.

This new manufacturing technique allows for almost infinite freedom of design and as bio-compatible materials can be used, offers new possibilities for customized medical products. Due to the manufacturing process, SLS-structures show a high level of roughness and therefore low strength. This is why peaks in strain and stress should be avoided in the design.

In 2003, (Breedveld 2003) introduced a snake-like kinematics based on a helical spring. A similar structure can be found in the prototype Endomina by Endo Tools Therapeutics. As a helical design shows a smooth load distribution in the material in bended pose, this seemed a good approach for a laser sintered snake-like structure.

A helical structure that fulfills the requirements for an SLS design very well was shown by (Roppenecker 2012). In his work, four tendons are attached to the structure's tip and cause the structure to bend when a tendon is pulled. The resulting working space is similar to that found for a conventional endoscope. Nevertheless, unpublished FEM analysis showed instabilities like buckling. Although the working space is three dimensional, the possible motion is limited to a single plane for most poses.

The contribution of this paper is to overcome these limitations with a new design. The tendons are placed inside the structure and contours are introduced in between the loops for enhanced stability. Also the maneuverability is enhanced to all three dimensions in nearly any pose. With the new design, cables crossing the working space could be eliminated.

2. METHODS

To retain the functionality with tendons inside the structure, gaps between the helical loops are essential. Contours are introduced in between the loops, to avoid the reduction of the structure's longitudinal stiffness. These contours also guarantee for a predictable bending movement and allow for application of forces in any position. Fig. 2 shows a schematic view of the contours.

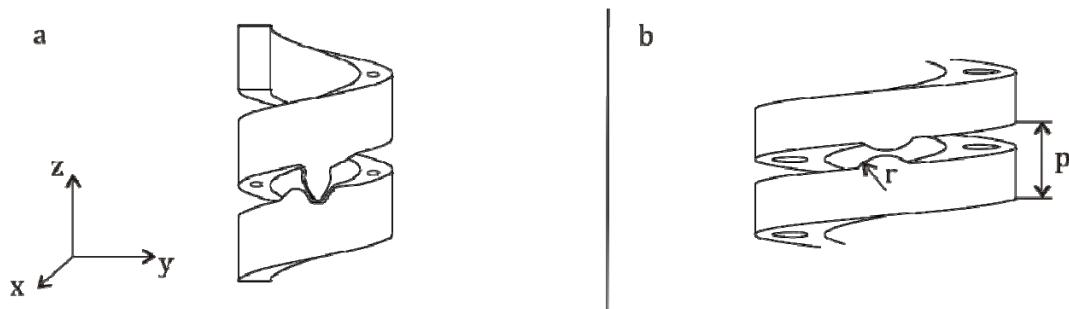


Fig. 2 schematic view of contours for the helix. Involute (a) and unrolling circles (b)

The SLS manufacturing process not only results a high roughness, but also high tolerances. Although a contour shaped like an involute (Fig. 2(a)) would be the best choice to guarantee precise movement, this is not applicable. Therefore, the contours were executed as two unrolling circles (Fig. 2(b)) with a radius r_{un} of half the helical pitch p . With this particular dimension, the total length of the structure will not change during actuation. For manipulators that make use of flexible instruments, this is a convenient functionality.

The contours' edges unnecessary for the unrolling movement were smoothed using splines. Fig. 3 shows the structure's finite element model in relaxed and bended pose.

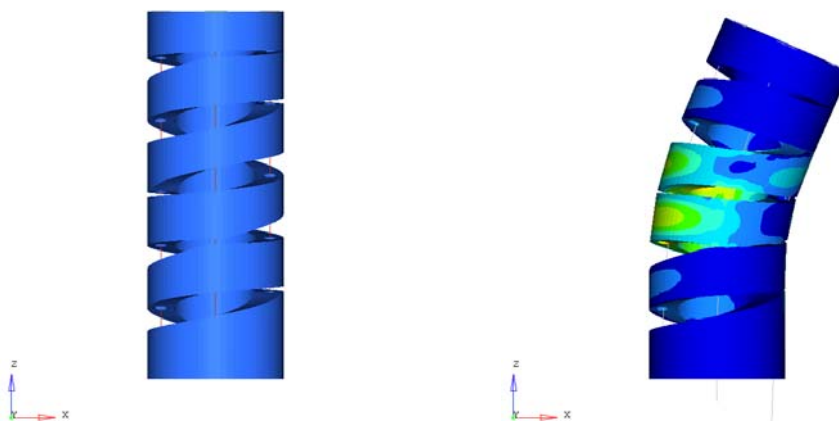


Fig. 3 FE-Model in relaxed (a) and bended pose (b)

To avoid FE simulation for different joint configurations and contour layouts, an analytical description for the structure's kinematic behavior is desirable. Therefore,

Denavit-Hartenberg parameters are derived for the solid state structure with the following two assumptions:

The unrolling contours are interpreted as joints and the distance along the length of the helix between two pairs of contours characterizes the offset between two joints. It is therefore specified by the DH parameter a . DH parameter Θ_i depends on the current tendon length ($\Theta_i = \Theta(d_t)_i$) and d is zero for all joints.

To achieve a kinematic behavior similar to an endoscopic tip or other snake-like structures, the contours are aligned in a distance of $3/2*\pi$ along the helix. The corresponding DH parameter is $a = 0.75*p$ with the helical pitch p .

All joints in xz - or yz -plane are actuated by one set of tendons each. Neglecting friction, this yields a constant curvature. All joints based on contours in xz -plane are called x -DOF in the following, as they result in a bending around the x -axis; all joints in yz -plane are called y -DOF, respectively. The DH parameter is $\alpha_i = -\pi/2$ for x -DOF-joints and $\alpha_i = \pi/2$ for y -DOF-joints.

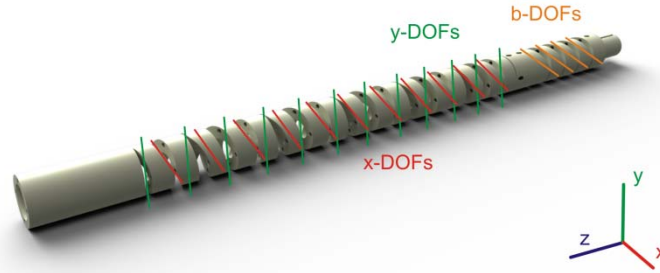


Fig. 4 Layout for the S-like bending with planar base joints

For the HVSPS, (Can 2012) suggested an S-like bending for the camera that allows for retroreflection. To gain this functionality, additional joints are introduced at the base. Tracking instruments during a sigma resection revealed that for an S-like camera kinematics, a planar working space for the base DOFs (b-DOFs) is sufficient. Thus, the base contours are introduced in an opposing layout in a distance of π along the helical structure as shown in Fig. 4. This results in a DH parameter $\alpha_i = 0$ and $a_i = p$ for all base joints. Fig. 4 shows the layout for an S-like bending with planar base joints.

Fig. 5(d) shows how the half bending angle β_h depends on the tendon length s . With $r_{un} \approx \frac{g}{2}$, the total bending angle β can be approximated

$$\beta \approx 2 \sin^{-1} \left(\frac{g-s}{2R_0} \right). \quad (1)$$

With the tendon displacement $d_t = g - 2s$, and $d_t = d_{t,max} = g$ the maximum bending angle is

$$\beta_{max} \approx 2 \sin^{-1} \left(\frac{g}{2R_0} \right). \quad (2)$$

To get the DH-parameter $\Theta(d_t)_i$, for any joint the exact relation of bending angle and tendon length is shown in Fig. 5. For a better understanding, one joint (Fig. 5(a)) is reduced to a simplified model (Fig. 5(b)). Again, β_h is the angle between the lower edge and a plane perpendicular to the tendon through the contact point.

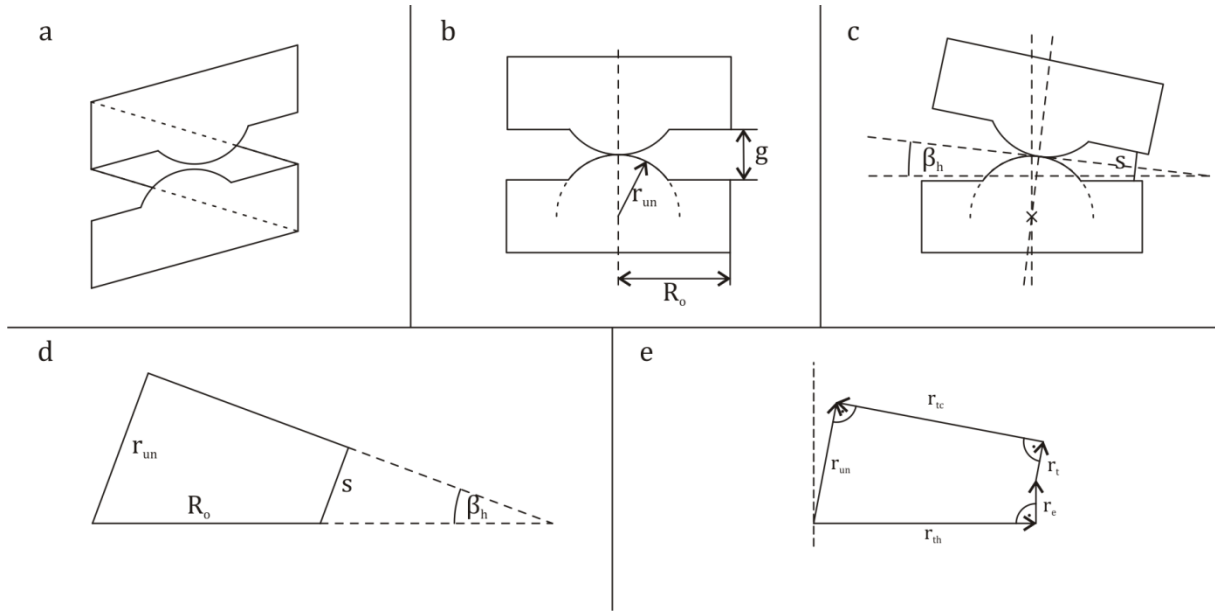


Fig. 5 Schematic view of helical joint (a), simplified model (b), half bending angle β_h and tendon lengths (c), approximation (d) and closed vector chain (e)

Fig. 5(c) shows the closed vector chain:

$$\vec{r}_{th} + \vec{r}_e + \vec{r}_t + \vec{r}_{tc} + \vec{r}_{un} = \vec{0} \quad (3)$$

Using the given values, we get the nonlinear equations

$$R_{th} + \left(\frac{s}{2} - r_{un}\right) \sin \beta_h + d_{tc} * \cos \beta_h = 0 \quad (4)$$

and

$$r_s + \left(\frac{s}{2} - r_{un}\right) \cos \beta_h + d_{tc} * \sin \beta_h = 0 \quad (5)$$

with $r_e = r_{un} - \frac{g}{2}$.

This system of nonlinear equations can be solved for the unknown β . After multiplication of (4) with $\cos(\beta_h)$ and (5) with $\sin(\beta_h)$ and addition of both equations we get

$$\beta_h = \beta_{em} - \beta_{ec} \quad (6)$$

with $\beta_{em} = \sin^{-1}\left(\frac{r_{un}-\frac{s}{2}}{\sqrt{R_{th}^2+r_e^2}}\right)$ and $\beta_{ec} = \tan^{-1}\left(\frac{r_e}{R_{th}}\right)$. In this expression, β_{ec} does not depend on the tendon length and is constant during actuation. It can be shown that this expression is not only valid for the simplified model (Fig. 5b) but also for the complete helix (Fig. 5(a)).

The resulting DH-parameter Θ_i for any joint i is

$$\theta_i = 2 \left(\sin^{-1}\left(\frac{r_{un}-s_i}{\sqrt{R_{th}^2+r_s^2}}\right) - \tan^{-1}\left(\frac{r_s}{R_{th}}\right) \right) \quad (7)$$

where $s_i = \frac{g-d_t}{2J_k}$ and J_k being the number of joints actuated by tendon k .

3. RESULTS

Fig. 6(0 shows the comparison of angle and tendon displacement in FEM (blue) and the analytical approach using Eq. (2) (red) as well as the linearized approximation $\alpha = \frac{g-s}{2R_o}$ (green). In the FEM approach, pretension was applied to get all contours in contact before bending. The tendon displacement for bending was $d_t = 2.2\text{mm}$. As the maximum bending angle per joint is small, the linearized approximation suits the FEM results sufficiently and will be used to describe the correlation of bending angle and tendon displacement in the future.

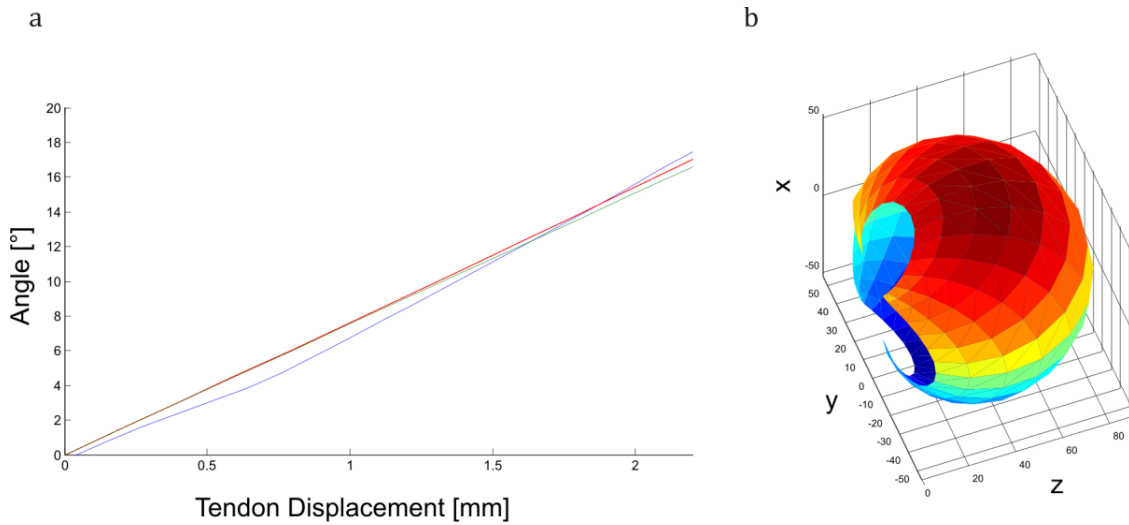


Fig. 6 comparison of bending angle with different approaches. FEM (blue), exact analytical approach (red) and linearized approximation (green) (a). Working space for the proposed design (b)

To get the camera assembled easily, we chose an inner radius of $R_i = 2$ mm for the helix. Manufacturing restrictions require a minimum wall thickness of $t_{\min} = 0.3$ mm. With the diameter for holes limited to $r_{h,\min} = 0.8$ mm this would allow for an outer radius $R_{o,\min} = R_i + 2 * t_{\min} + r_{h,\min} = 3.4$ mm. As we do not focus on miniaturization yet, we chose $R_o = 3.8$ mm. The resulting wall thickness of $t = 1.8$ mm leaves enough room for the tendons to be conducted inside.

To limit the strain and to get a maximum bending angle per joint that can be linearized with small-angle approximation, we chose $g = 1.1$ mm. This results in a maximum bending angle $\beta_{\max} \approx 16.6^\circ$ per joint. Due to manufacturing restrictions, a gap of $d_g = 0.2$ mm is left in between any pair of contours which is closed after pretension is applied.

The homogeneous load distribution throughout the material led to a very high strength. Until today, none of the prototypes has been damaged due to strain.

By actuating only the x-DOFs and y-DOFs a working space as shown in Fig. 6b can be predicted using DH-parameters for the given design.

4. DISCUSSION

The FEM model showed linear behavior of bending angle versus tendon displacement. Even the linearized approximated approach showed good correlation with FEM data.

The tendons could be used to maneuver the camera as expected. First tests showed a good match with the predicted working space using DH-parameters and a very high strength. Nevertheless, stick-slip effects as known in many tendon driven mechanics occurred.

Although the powder PA2200 used for SLS is certificated as biocompatible according to ISO 10993-1, the process itself is not yet certified. Nevertheless, tests to autoclave the material were promising. Custom-tailored kinematics and instruments are not necessary for every surgical intervention, even more. As bending units are expensive and very difficult to manufacture and hard to obtain, the method presented here allowed to try out several configurations and to even use them for in vivo testing. In an interdisciplinary project like this, SLS provides the opportunity to try out optimized joint configurations and discuss the mechanics with engineers, endoscopists and surgeons within a short period of time.

5. CONCLUSION

A new design method for snake-like kinematics manufactured by SLS was presented. The new design's functionality could be validated with a camera orientation unit. A smooth curvature which is essential for the use of flexible endoscopic instruments could be obtained. This will provide the opportunity to even design manipulators using the proposed method. The kinematic behavior was described in an analytical way and compared to FEM data. Based on the good match, the structure's working space can be described using DH-parameters. This fast model can be the base for an optimized joint configuration.

As there are many approaches to design new SP or NOTES-Manipulators for flexible instruments, the time between design and test can be reduced using SLS. With the analytical approach, design parameters like joint configuration can be optimized and the new design can be manufactured literally overnight. The proposed kinematics shows a good alternative to expensive and customized snake-like kinematics.

In the future, there will be a test setup for comparison of simulation and prototype. Autoclave tests are ongoing at the moment. In the current generation of HVSPS, the prototype was included and will be used for in vivo testing.

To control the camera's position, Fiber Bragg sensors will be integrated.

Simulation with data of tracked instruments during a sigma resection showed, that an alternating layout of x- and y-DOFs is not essential. As the four base joints showed the most precise behavior due to their opposing layout, the next prototype will be designed with a serial layout concerning x- and y-DOFs.

REFERENCES

- Breedveld P., Sheltes P., Blom, E.M., Verheij J.E.I (2005), "A new, easily miniaturized steerable endoscope", *IEEE Engineering in Medicine and Biology* (6), 40-47.
- Can, S., Jensen, B., Dean-Leon, E. Staub, C, Knoll, A., Fiolka, A. Schneider, A., Meining, A. and Feussner, H. (2012), "Kinematics, control and workspace analysis of a Bowden wire actuated manipulator for minimally invasive single-port surgery", *IEEE Int. Conference on Robotics and Biomimetics*.
- Dario P., Carrozza M., Marcacci M., D'Attanasio S., Magnani B., Tonet O. & Megali G. (2000), "A novel mechatronic tool for computer-assisted arthroscopy", *Information*

- Technology in Biomedicine. IEEE Transactions on 4(1), 15--29.
- Degani A., Choset H., Wolf A. & Zenati M. (2006), „Highly articulated robotic probe for minimally invasive surgery“, in 'Robotics and Automation, 2006. ICRA 2006. Proceedings 2006 IEEE International Conference on', pp. 4167 -4172.
- Ding J., Xu K., Goldman R., Allen P., Fowler D. & Simaan N. (2010), „Design, simulation and evaluation of kinematic alternatives for Insertable Robotic Effectors Platforms in Single Port Access Surgery“, in 'Robotics and Automation (ICRA), 2010 IEEE International Conference on', pp. 1053 -1058.
- Peirs J., Brussel H. V., Reynaerts D. & Gerssem G. D. (2002), „A flexible distal tip with two degrees of freedom for enhanced dexterity in endoscopic robot surgery“, 13th Micromechanics Europe Workshop 13, 271--274.
- Roppenecker D.B, Meining A., Horst G., Ulbrich H., Lueth T.C. (2012) “Interdisciplinary development of a Single-Port Robot”, Proceedings of the 2012 IEEE Int. Conference on Robotics and Biomimetics: 612-617.
- Weede O., Dittrich F., Woern H., Jensen B., Knoll A., Wilhelm D., Kranzfelder M., Schneider A. & Feussner H. (2012), „Workflow Analysis and Surgical Phase Recognition in Minimally Invasive Surgery“, in '2012 IEEE International Conference on Robotics and Biomimetics (ROBIO 2012), December 11-14, 2012, Guangzhou, China'.